Scientific Research Publishing

Open Journal of Applied Sciences, 2024, 14, 687-706
https://www.scirp.org/journal/ojapps
ISSN Online: 2165-3925
ISSN Print: 2165-3917

Optimization of Tin-Doped Hybrid Perovskite Solar Cells

Bakary Coulibaly Abou[1,2*], Ahou Florentine Kokora[1,2], Desiré Meledje[1,2,3], Boko Aka[1,2,3], Bernabé Mari Soucase[4]

[1]IREN (Institut de Recherche sur les Energies Nouvelles, Abidjan, Cote d'Ivoire
[2]Unité de Formation et de Recherche des Sciences Fondamentales Appliquées (UFRSFA), Universite Nangui Abrogoua, Abidjan, Cote d'Ivoire
[3]Laboratoire de Physiques Fondamentales Appliquées (LPFA), Université Nangui Abrogoua, Abidjan, Cote d'Ivoire
[4]Institut de Disseny i Fabricació, Universitat Politècnica., València, Spain
Email: *kaliema1010@gmail.com, kokoraflorentine@gmail.com, desiremeledje@gmail.com, bokom2010@gmail.com, bmari@fis.upv.es

How to cite this paper: Abou, B.C., Kokora, A.F., Meledje, D., Aka, B. and Soucase, B.M. (2024) Optimization of Tin-Doped Hybrid Perovskite Solar Cells. *Open Journal of Applied Sciences*, **14**, 687-706.
https://doi.org/10.4236/ojapps.2024.143049

Received: February 10, 2024
Accepted: March 24, 2024
Published: March 27, 2024

Abstract

Perovskites are a category of materials with a unique crystal structure that allows them to absorb sunlight efficiently. This efficiency is particularly high in the case of $CH_3NH_3Pb_{1-x}Sn_xI_3$ mixed perovskites. The combination of lead (Pb) and tin (Sn) in this matrix provides a broad spectrum of sunlight absorption, enabling the generation of a larger voltage and, subsequently, increased power. The primary objective in solar cell development is to maximize the conversion of sunlight into electricity. Mixed perovskites like $CH_3NH_3Pb_{1-x}Sn_xI_3$ have demonstrated significant potential in this regard. Their tunable bandgap, courtesy of varying the Pb: Sn ratio, allows for the optimization of sunlight absorption. The result is solar cells that surpass many conventional counterparts in terms of energy efficiency. Another significant advantage of these mixed perovskite solar cells is their cost-effectiveness. They can be manufactured using solution-based processes, which are less expensive than the high-vacuum methods required for traditional silicon solar cells. While the prospects for mixed perovskite solar cells are undeniably promising, there are concerns about the toxicity of lead, a key component of these cells. Lead is known to have harmful effects on the environment and health. The aim of our work is to reduce or eliminate lead toxicity in the perovskite cell while maintaining its efficiency. Thus, in a theoretical and experimental approach, we obtained following efficiencies of samples: $CH_3NH_3PbI_3$ (22.49%) $CH_3NH_3Pb_{0.75}Sn_{0.25}I_3$ (22.72%), $CH_3NH_3Pb_{0.5}Sn_{0.5}I_3$ (23.00%) $CH_3NH_3Pb_{0.25}Sn_{0.75}I_3$ (22.61%), $CH_3NH_3SnI_3$ (22.38%). Doping with 50% tin gives the highest result (23.00%). By replacing a fraction of the lead with tin, the research aims to reduce the environmental footprint of the cells while

maintaining their high performance. However, the challenge is to achieve a balance that does not compromise performance while reducing toxicity.

Keywords

Cost, Efficiency, Lead/Tin, Perovskite, Toxicity

1. Introduction

The Sun, an almost unlimited source of energy, is the source of an impressive number of biological effects that participate directly or indirectly in animal and plant life: it provides heat, allows photosynthesis, vision, conditions biological rhythms, etc. The originality of photovoltaic energy is that it is the direct conversion of sunlight into electricity. And when you know that the total energy contribution of the sun on the planet is several thousand times greater than our overall energy consumption [1], you can see the importance of such an approach. Very recent, the importance of renewable energy and amongst it solar photovoltaic electricity for mitigating Climate Change was highlighted by a special report of the Intergovernmental Panel for Climate Change (IPCC) [2]. Despite its abundance, solar energy remains largely unexploited and unused because of the high cost of its production. The conversion of solar light energy is mainly carried out by the material silicon. The processing of silicon is very energy-intensive and expensive. Much research is being carried out to find cheaper alternatives to silicon.

In the recent decades, perovskite photovoltaic cells are a great promise solution to convert solar energy into electric energy [3]. The power conversion efficiencies of solar energy into electrical energy in perovskite solar cells are now close to those of the best traditional silicon solar cells [4]. But standard perovskite cells contain lead, a heavy metal that is toxic to the environment and can seriously damage health because the lead can dissolve in water. This solubility in water and other solvents is a great advantage because the synthesis of perovskite solar cells is simpler and cheaper [5]. But the solubility of lead in water can become a real environmental and health problem when the panel breaks. Lead must therefore be collected before it reaches the ground and its recycling must be possible. This drawback has been the subject of much research. For authorities and certification, it is a serious obstacle to approve the large-scale production and commercialization of perovskite photovoltaic cells [6].

Alternative perovskite compositions offer the opportunity to replace lead with non-toxic metals. Lead can be directly replaced by tin. Several investigations to solve the toxicity problem of lead-based perovskite solar cells are focused on substitute lead with tin. Indeed, tin is among the most promising candidates to replace Pb as they both belong to the IVA group and have isoelectronic configurations. Using DFT, hybrid DFT and QSGW for electronic structure calculations, Mosconi *et al.* [7] and Goyal *et al.* [8] obtained the best percentage of

doping. What can be the result obtained by simulation with SCAPS-1D? But the development of Sn-based perovskites is compromised by their instability. This defect is explained by the fact that tin oxidizes more easily than lead. Indeed, during the synthesis of the perovskite, some ions Sn^{2+} transforms into ions Sn^{4+} making the material less efficient as a photoconductor. The wit to avoid this nasty situation is to add tin sulphide SnF_2 which reduces or prevents this oxidation [9]. In this work, we seek to determine the proportion of lead that should be replaced by tin in order to obtain a better material for photovoltaic applications

2. Experimental Detail

2.1. Description of the Crystal Structure

The perovskite lattice consists of corner-sharing lead (Pb) or tin (Sn) octahedra, encapsulating the organic methylammonium (CH_3NH_3) cations within the interstitial spaces (**Figure 1**) [10]. The substitution of tin for lead in this compound (x represents the degree of substitution) introduces alloying effects, impacting both the electronic and structural properties.

The crystal structure undergoes a transition from a tetragonal to a cubic phase with increasing tin content, influencing the material's bandgap and optical properties [11]. This phase transition has crucial implications for the solar cell performance of these materials. The organic cations play a crucial role in stabilizing the perovskite structure, contributing to its remarkable stability and electronic characteristics. Understanding the crystal structure at the atomic level is pivotal for tailoring the properties of $CH_3NH_3Pb_{(1-x)}Sn_xI_3$, optimizing its performance, and advancing its applications in solar cells and other emerging technologies [12].

2.2. Simulation of Device and Modeling

The numerical study of the proposed solar cell structure is performed using Solar Cell Capacitance Simulation Software (SCAPS) (version 3.3.10). SCAPS (solar cell capacitance simulator) is a numerical simulation software for of heterojunction thin film solar cells. It has been developed at the University of Ghent in Belgium with LabWindows/CVI from National Instruments by Marc Burgelman *et al.* [13].

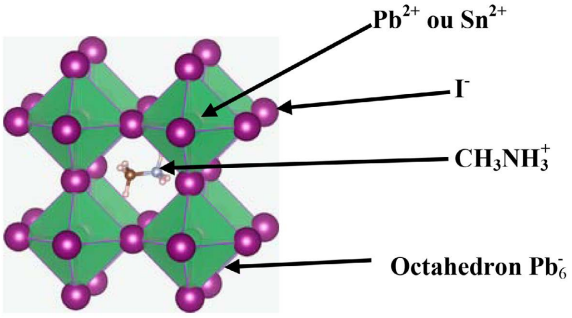

Figure 1. Crystal structure of $CH_3NH_3Pb_{(1-x)}Sn_xI_3$.

The hybrid perovskites are characterized by a direct gap and a high absorption coefficient [14]. The absorption coefficient of the $MAPbI_3$ perovskite is about 1.5 × 10^4 cm^{-1} at 550 nm close to that of materials usually used in photovoltaics. Hybrid perovskite $MAPbI_3$ has a gap between 1.5 and 1.55 eV [15] well placed in the field of photovoltaic applications [16] [17]. The gap of the material varies according to its composition. The incorporation of x ratio tin reduces the gap from 1.55 eV to 1.17 eV and it increases slightly to 1.3 eV (**Figure 2**) [18].

The simulation was done under the illumination of 1000 W/m^2, at 300 K and an air mass of AM 1.5 G. The values of the device and material parameters that are adopted from theories, experiments and literature are summarized in **Table 1** below.

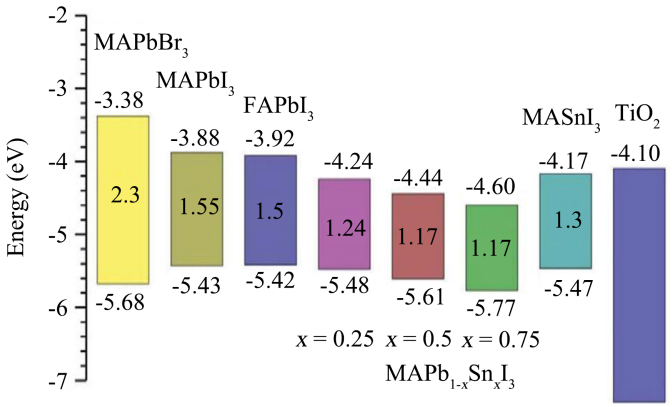

Figure 2. Schematic energy level diagram of $MAPbBr_3$, $MAPbI_3$, $FAPbI_3$ $MAPb_xSn_xI_3$ and $MASnI_3$ along with TiO_2. Data for $MAPb_{1-x}Sn_xI_3$ (x = 0; 0.25; 0.5; 0.75 and 1).

Table 1. Simulation parameters of perovskite solar cells.

Material Properties	$MAPb_xSn_{1-x}I_3$	Spiro-OMETAD	TiO_2	FTO
X (μm)	0.3	0.05	0.03	0.5
Eg (eV)	(see **Figure 2**)	3.0 [19]	3.3 [20]	3.5 [20]
χ (eV)	3.9 [21]	2.45 [19]	4.4 [20]	4 [20]
εr	6.5 [22]	3 [19]	9 [20]	9 [20]
Nc (cm^{-3})	2×10^{18}	2×10^{18} [23]	2×10^{18}	2×10^{18}
Nv (cm^{-3})	10^{19}	10^{19}	10^{19}	1.8×10^{18}
vn ($cm \cdot s^{-1}$)	10^7	10^7	10^7	10^7
vh ($cm \cdot s^{-1}$)	10^7	10^7	10^7	10^7
μn/μh ($cm^2/v.s$)	2.0/2.0 [24]	$2 \times 10^4/2 \times 10^4$ [22]	20/10 [20]	20/10 [20]
Nd (cm^{-3})	varied	0	10^{16}	2×10^{19}
Na (cm^{-3})	0	10^{18}	0	0
Nt (cm^{-3})	10^{14}	10^{14}	10^{14}	10^{14}
Et (eV)/distribution	0.7 eV above eV	0.1 eV above eV	0.6 eV above eV	0.6 eV above eV

2.3. Synthesis of Perovskite

Two solutions containing the perovskite precursors $CH_3NH_3PbI_3$ ($MAPbI_3$) and perovskite $CH_3NH_3SnI_3$ ($MASnI_3$) are prepared. The perovskite $MAPbI_3$ is obtained by mixing the precursors: Methylammonium iodide (CH_3NH_3I: MAI), lead iodide (PbI_2, 99%) and the perovskite $MASnI_3$ with the precursors: Methylammonium iodide (CH_3NH_3I: MAI), tin iodide (SnI_2, 99%) All chemicals were bought from Sigma-Aldrich. The precursors were mixed in a 1:1 (stoichiometric) molar ratio in a polar aprotic solvent (Dimethylformamide (DMF, 99.9%) and Dimethylsulfoxide (DMSO, 99.9%) for 10 min to 15 min at room temperature until a clear solution was obtained (Figure 3). These solutions are then used to obtain the solutions $MAPb_{0.25}Sn_{0.75}I_3$, $MAPb_{0.5}Sn_{0.5}I_3$, $MAPb_{0.75}Sn_{0.25}I_3$. The glass substrate used is Fluorine-doped Tin oxide (FTO). The glass substrate was consecutively cleaned with diluted detergent, deionized water, acetone, and ethyl alcohol. The FTO glass was dried with an N_2 stream and treated with UV-ozone for 15 min to residual organic contaminants. 0.2 ml of each solution is deposited on the FTO substrates by spin-coating (2000 rpm - 3000 rpm, 2 s - 20 s). During the rotation of the substrate, a few drops of chlorobenzene solution are applied to evaporate the solvents, then the perovskite crystallizes. After deposition an annealing is necessary to complete the crystallization and evaporate the solvent residues. Then the deposit is annealed on a hot plate for 10 minutes at 70˚C to form perovskite film (Figure 4).

- **Synthesis of the perovskite solution**

3. The Goldschmidt Tolerance Factor

The Goldschmidt Tolerance Factor is a critical parameter in the study and design of perovskite materials, especially in the context of perovskite solar cells and

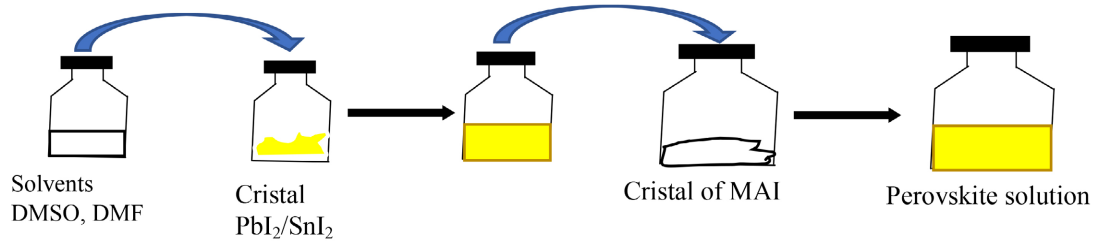

Figure 3. Perovskite solution synthesisprocesses.

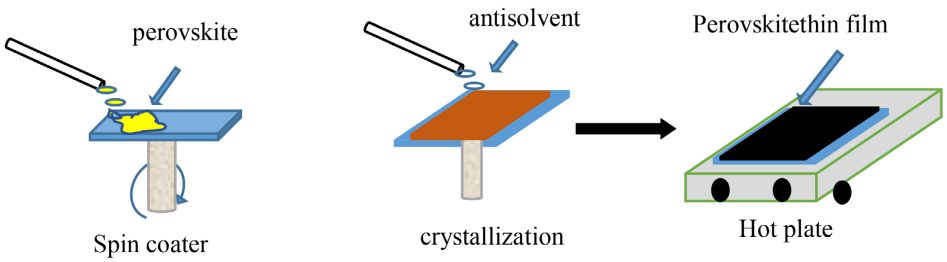

Figure 4. Perovskite film production processes.

other applications in materials science. Its importance lies in its ability to provide insights into the structural stability, phase transitions, and functional properties of perovskite materials. The Goldschmidt Tolerance Factor helps determine whether a given composition is likely to form a stable perovskite crystal structure. Perovskites are known for their unique crystal symmetry, and deviations from this structure can significantly affect their properties. A proper Tolerance Factor value within a certain range (typically 0.9 to 1) ensures that the crystal structure remains stable, which is essential for various applications [25]. In the field of perovskite solar cells, the Tolerance Factor is of particular importance. It can impact the efficiency of energy conversion by influencing the charge carrier dynamics and the ability of the material to absorb and convert sunlight into electricity. A suitable Tolerance Factor is essential for achieving high-efficiency solar cells [26].

The Tolerance Factor can also be a factor in addressing environmental and safety concerns. For instance, the substitution of toxic elements with less toxic ones can affect the Tolerance Factor and may lead to improved materials with reduced environmental impact. $MAPb_xSn_{1-x}I_3$ is a mixed perovskite whose the Goldschmidt tolerance factor formula [10] is:

$$t = \frac{R_{MA^+} + R_{I^-}}{\sqrt{2}\left[(1-x)R_{Pb^{2+}} + xR_{Sn^{2+}} + R_{I^-}\right]} \quad (1)$$

- R_{MA^+} (Ionic radius of $MA^+ = CH_3NH_3^+$) ≈ 1.64 Å (angstroms)
- $R_{Pb^{2+}}$ (Ionic radius of Pb^{2+}) ≈ 1.19 Å
- $R_{Sn^{2+}}$ (Ionic radius of Sn^{2+}) ≈ 1.06 Å
- R_{I^-} (Ionic radius of I^-) ≈ 2.20 Å

The calculated values for each compound can be found in **Table 2** below.

As we move from $MAPbI_3$ to $MASnI_3$, we observe a systematic increase in the Goldschmidt Tolerance Factor (t). This trend suggests that as the proportion of Sn in the crystal structure increases, the structural distortion within the perovskite lattice decreases. In other words, Sn seems to be a better fit for the crystal structure compared to Pb in this context. A higher t value indicates a closer match between the ionic radii of the cations and anions, which results in a more stable crystal lattice with reduced distortion. Therefore, the perovskite structure becomes more stable and less likely to undergo phase transitions or degradation. The structural properties of perovskite materials play a crucial role in their optoelectronic properties [27]. A more stable crystal lattice with less distortion can lead to better performance in various applications, such as solar cells, LEDs, and photodetectors [28]. These results can inform materials scientists and engineers working on perovskite-based devices. For example, if high stability and minimal

Table 2. Goldschmidt tolerance factors.

	$MAPbI_3$	$MAPb_{0.75}Sn_{0.25}I_3$	$MAPb_{0.5}Sn_{0.5}I_3$	$MAPb_{0.25}Sn_{0.75}I_3$	$MASnI_3$
Goldschmidt Tolerance Factor	$t = 0.889$	$t = 0.895$	$t = 0.902$	$t = 0.909$	$t = 0.915$

distortion are desired, $MASnI_3$ might be a more suitable choice than $MAPbI_3$. The systematic increase in the Goldschmidt Tolerance Factor as Sn replaces Pb suggests that Sn-containing perovskites may offer advantages in terms of structural stability, which can have implications for various technological applications. These results contribute to our understanding of perovskite materials and guide future research and development efforts in this field.

4. Results and Discussion

4.1. Curves JV

Figure 5 below shows the current-voltage (JV) characteristics, measured under AM1.5 illumination of the types of perovskite material synthesised. The Current-voltage (J-V) measurement can be used to characterize a solar cell. Different characteristic parameters can be extracted from such a measurement: short-circuit current (J_{SC}), open circuit voltage (V_{OC}), fill factor (FF) and conversion efficiency (η) of the cell. When we introduce Sn (tin) into the crystal lattice of $CH_3NH_3Pb_{(1-x)}Sn_xI_3$ materials, it creates a solid solution where Pb (lead) ions are partially replaced by Sn ions. This substitution modifies the composition of the material, which can carry away to changes in its properties. The modification in the crystal lattice will affect the physical properties of the material, including its optical, electrical, and structural characteristics [29].

Pure $CH_3NH_3PbI_3$ serves as the reference material in this study. It exhibits relatively high Voc and moderate Jsc, resulting in a decent overall efficiency of 22.49%. The fill factor (FF) at 63.71% indicates that there is possibility to improve the collection and extraction of charges in the cell. With the introduction of 25% tin (x = 0.25), we observe a improvement in Jsc (43.02 mA/cm^2) and 31.25 mA/cm^2 for $CH_3NH_3PbI_3$, indicating enhanced light absorption and charge carrier generation. However, his Voc is smaller than that $CH_3NH_3PbI_3$, which

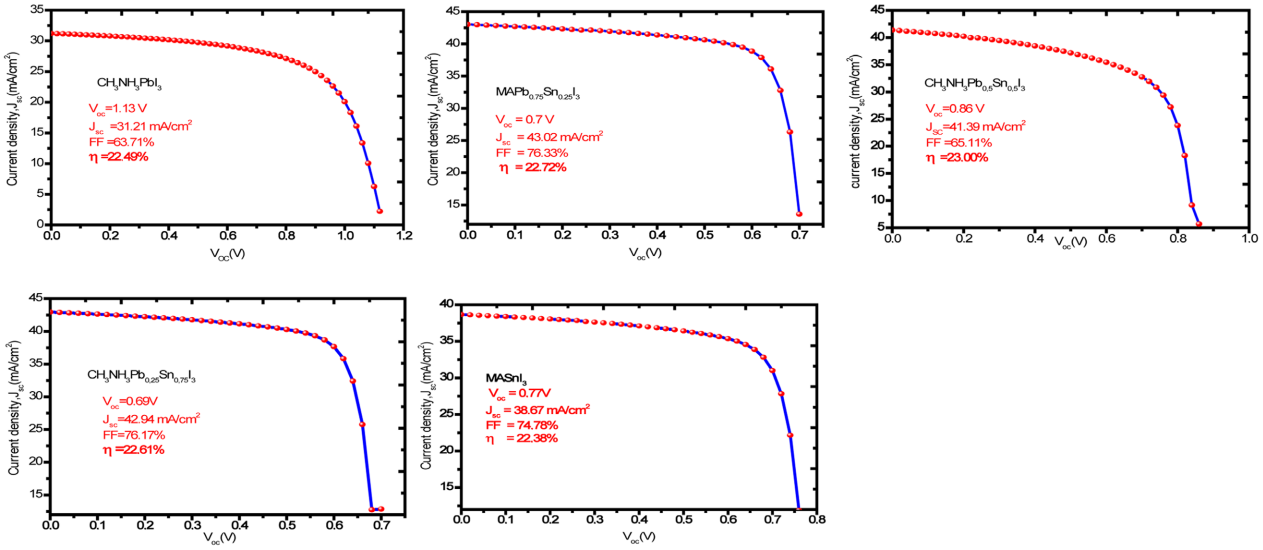

Figure 5. J-V curve of different perovskite solar cells.

could be attributed to charge recombination or bandgap shift due to tin incorporation. Nonetheless, the overall efficiency improves slightly to 22.72%, primarily due to the increased Jsc and FF (76.33%). At x = 0.5, we observe a further improvement in Voc (0.85 V) while maintaining a high Jsc (43.19 mA/cm^2). At x = 0.5, we observe a slight increase in Voc (0.85 V) compared with the previous compound (x = 0.25), while maintaining a high Jsc (43.19 mA/cm^2). The FF, however, drops to 65.11%, indicating potential challenges in charge transport or recombination. Despite this, the overall efficiency reaches 23%, making it the most efficient composition. When the tin composition reaches x = 0.75, the Voc drops significantly to 0.69 V. This suggests a more pronounced influence of tin on the perovskite bandgap, leading to lower Voc values. Nonetheless, the Jsc remains high (42.94 mA/cm^2), and the FF improves considerably to 76.17%, leading to a relatively overall efficiency of 22.61%. At x = 1, the perovskite material becomes pure $CH_3NH_3SnI_3$ without any lead (Pb) content. We observe a similar trend as with increasing tin content: a drop in Voc (0.77 V) and a moderate Jsc (38.67 mA/cm^2). The FF remains relatively high (74.78%), leading to an overall efficiency of 22.38%.

The results show that the addition of tin to the $CH_3NH_3PbI_3$ perovskite affects the solar cell's performance. As the tin content increases, the Voc decreases, likely due to changes in the bandgap and charge recombination processes. However, the Jsc remains high, indicating improved light absorption. The FF varies throughout the tin composition range, suggesting challenges in charge transport and extraction at certain compositions.

The highest overall efficiency is achieved at x = 0.5, where the combination of improved Voc and high Jsc contributes to the superior performance. However, as the tin content approaches x = 1, the efficiency starts to decrease due to the reduced Voc. The analysis of $CH_3NH_3Pb_{(1-x)}Sn_xI_3$ perovskite materials with varying Sn content (x) reveals the crucial role of composition in determining the photovoltaic performance of solar cells. The introduction of Sn enhances light absorption and charge generation, resulting in higher short-circuit current densities (Jsc). The fill factor (FF) demonstrates the effective charge extraction and reduced recombination losses, contributing to improved efficiency (η). The V_{OC} is affected by the bandgap tuning with Sn content, and a trade-off exists between Voc and Jsc. These findings underscore the significance of material engineering in advancing perovskite solar cell technology and accelerating the transition to sustainable energy solutions.

4.2. Effect of Absorber Layer Thickness

In a solar cell, the conversion of light energy into electrical energy is not complete. Different losses influence the output parameters of a cell. These are in most cases due to the nature of the material and the technology used. One of the parameters that considerably modifies the performance of the cells is the variation of the thickness of absorbent layer.

The given curves (Figure 6) provide insight into the open-circuit voltage (V_{OC}) of different perovskite materials with varying lead-tin compositions and thicknesses. Across all compositions, as the thickness of the perovskite layer increases, V_{OC} appears to rise, albeit at diminishing increments. This could be attributed to the decrease in the recombination rate with thickness. The highest V_{OC} are obtained for MAPbI3 with the highest lead content. As the lead content decreases and tin content increases, the V_{OC} generally reduces. This pure lead-based perovskite shows the highest V_{OC} across all thicknesses. It starts at 1.09 V at 100 nm and reaches 1.18 V at 1000 nm. The increase in V_{OC} with thickness is evident, although the rate of increase tapers off. For instance, the difference in V_{OC} from 100 nm to 200 nm is 0.02 V, but from 900 nm to 1000 nm, it's only 0.015 V. This could suggest a saturation point in the V_{OC} value for this material at thicker layers. The materials with increasing tin content (decreasing lead content) display progressively lower V_{OC} values. For instance, at 100 nm, $MAPbI_3$ has a V_{OC} of 1.09 V, whereas $MASnI_3$ (with no lead) stands at 0.75 V. This observation aligns with the understanding that tin-based perovskites usually have lower V_{OC} values compared to their lead-based counterparts due to differences in their band gaps and other intrinsic material properties. The V_{OC} increments are non-linear as thickness increases. This is especially visible in the compositions with higher tin content. For example, in $MAPb_{0.5}Sn_{0.5}I_3$, the V_{OC} jumps by 0.026 V between 100 nm and 200 nm, but only by 0.006 V between 900 nm and 1000 nm. As the thickness increases, the rate of V_{OC} increment decreases for all materials, suggesting that each of these perovskite compositions might have an optimal thickness after which further increases in thickness wouldn't significantly enhance V_{OC}.

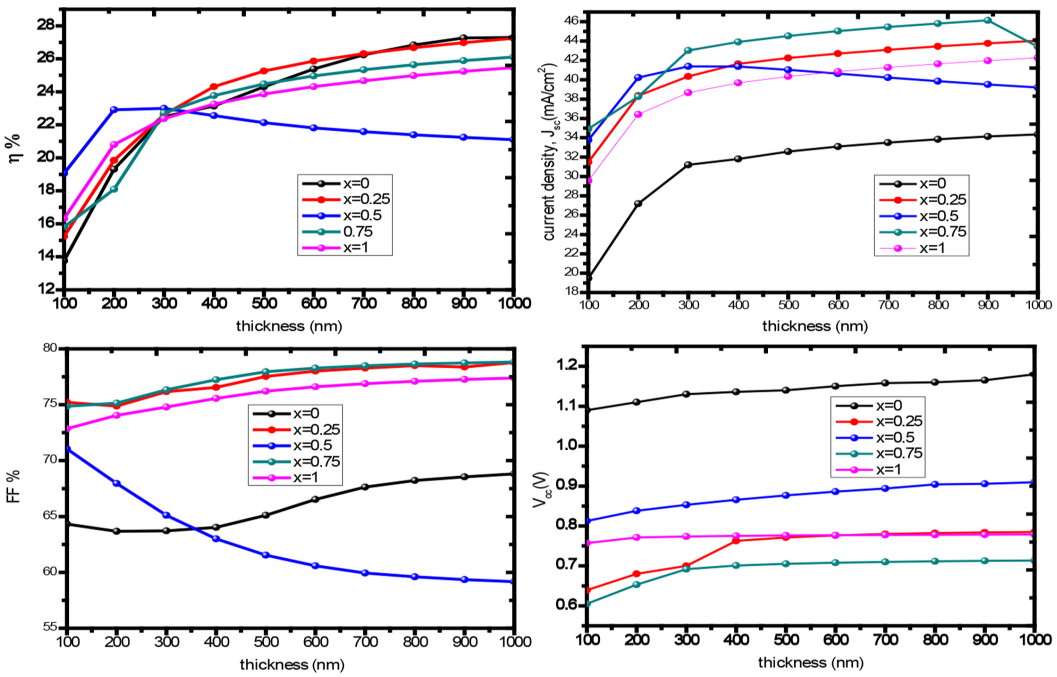

Figure 6. Curve of thinkness variation.

While increasing thickness does improve V_{OC}, it also means using more material. From a manufacturing and cost perspective, it would be crucial to balance the V_{OC} gains with the amount of material utilized. It's worth noting that tin-based perovskites, despite their lesser V_{OC} when compared to lead-based ones, are often researched for their potential lower toxicity.

The first notable trend is the general increase in efficiency with increasing film thickness for all compositions. This can be attributed to the fact that thicker films have a greater chance of capturing more photons, thus leading to improved light absorption and subsequently higher power conversion efficiency. This trend is consistent with the principles of light absorption and electron-hole pair generation within the perovskite material.

For the $MAPbI_3$ composition, the efficiency starts at 13.76% for a film thickness of 100 nm and gradually increases to 27.29% for a film thickness of 1000 nm. The increase in efficiency is significant, particularly from 100 nm to 400 nm, after which the efficiency gains become more gradual. This trend underscores the importance of optimizing film thickness to strike a balance between light absorption and charge carrier extraction efficiency.

When comparing the different compositions, there are interesting observations. The compositions containing tin (Sn) substitutions, such as $MAPb_{0.5}Sn_{0.5I3}$, exhibit generally higher efficiencies compared to pure $MAPbI_3$. This could be attributed to the beneficial effects of tin on the material's electronic properties, leading to improved charge transport and reduced recombination rates. This trend is particularly evident at greater film thicknesses, where the Sn-containing compositions consistently outperform $MAPbI_3$. The enhancement in efficiency is most pronounced for $MAPb_{0.5}Sn_{0.5I3}$, which achieves the highest efficiency values among the tin-containing compositions.

$MASnI_3$, the composition composed entirely of tin, shows competitive efficiency values compared to the other compositions. This highlights the potential of tin-based perovskite materials as promising candidates for efficient solar cells. The efficiencies of $MASnI_3$ are comparable to or even slightly better than those of the other compositions in some cases, indicating the potential for tin-based perovskites to be a viable alternative to lead-based ones.

In terms of film thickness optimization, it's important to note that while thicker films generally lead to higher efficiencies, there is an upper limit beyond which the gains become marginal or even plateau [30]. This could be due to factors such as increased charge recombination in thicker films, as well as challenges in maintaining uniformity and stability in very thick films. Therefore, there's a trade-off between maximizing light absorption through thickness and maintaining efficient charge extraction and transport.

The overall trend of increasing efficiency with greater film thickness is consistent with the principles of light absorption and charge carrier generation [31]. Additionally, the influence of tin substitutions in enhancing efficiency is evident, particularly at larger film thicknesses. $MASnI_3$'s competitive performance sug-

gests the potential for tin-based perovskites as alternatives to lead-based counterparts. This analysis underscores the importance of optimizing film thickness and composition to achieve the highest possible efficiency while considering factors like charge transport and recombination. Future research could delve deeper into the underlying mechanisms driving these trends and explore strategies for further efficiency improvements and material stability.

5. Effect of Doping Concentration

Doping is a common technique used in various fields, such as electronics and materials science, to modify the properties of a material by introducing impurities [32]. The efficiency of the process is being measured across different levels of doping, represented by varying values of x, ranging from 1 to 0 (**Figure 7**). Efficiency results indicate the performance of each configuration under different doping concentrations. It's important to note that efficiency is a crucial parameter in solar cells, representing the ability of the cell to convert incoming sunlight into electrical energy.

The efficiency of $CH_3NH_3PbI_3$ generally increases with higher doping concentrations. There is a peak efficiency at the doping concentration of 10^{16} cm^2, after which the efficiency starts to decline. The introduction of Sn in the perovskite structure affects the efficiency differently depending on the ratio. Configurations with higher Sn content (e.g., $CH_3NH_3Pb_{0.25}Sn_{0.75}I_3$) show a decrease in efficiency compared to $CH_3NH_3PbI_3$, especially at lower doping concentrations.

$CH_3NH_3Pb_{0.5}Sn_{0.5}I_3$ exhibits an efficiency trend similar to $CH_3NH_3PbI_3$, while $CH_3NH_3Pb_{0.75}Sn_{0.25}I_3$ shows mixed results. $CH_3NH_3SnI_3$ generally demonstrates competitive efficiency, comparable to $CH_3NH_3PbI_3$, and outperforms some of the Sn-doped configurations at certain doping concentrations. The efficiency tends to increase with the doping concentration up to a certain point.

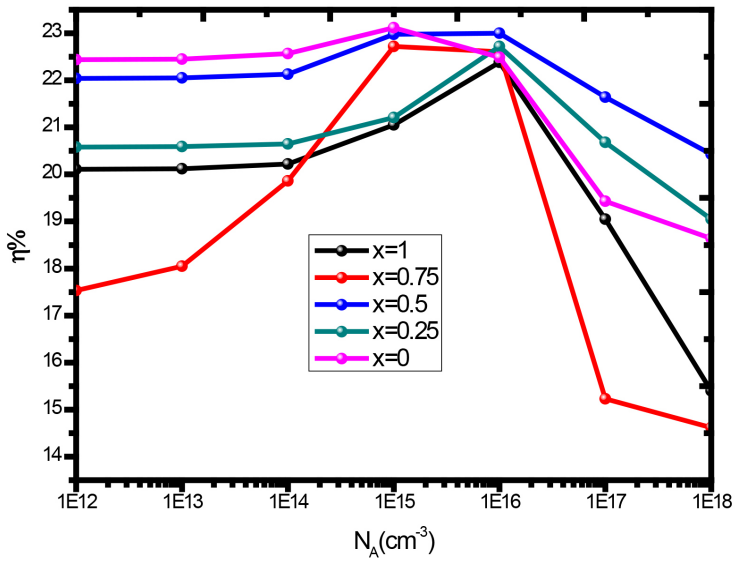

Figure 7. Curves of doping concentration variation.

Beyond a specific doping concentration (around 10^{16} cm^{-3}), the efficiency either stabilizes or decreases, suggesting an optimal doping level for each configuration. A doping concentration higher than 10^{16} cm^{-3} creates recombination defects affecting the performance of the system, resulting in a decrease of efficiency for each of the materials. Each configuration responds differently to doping, indicating that the choice of materials and their ratios is crucial for optimizing the performance of perovskite solar cells.

6. Photoluminescence

We used a spectrometer Ocean Optics HR4000 connected to a back-thinned Si-CCD Hamamatsu sensor with a He-Cd laser at 405 nm as an emission source.

The curves present a comparative analysis of photoluminescence (PL) intensity peaks observed at different temperatures for the three perovskite compounds: $CH_3NH_3PbI_3$, $CH_3NH_3Pb_{0.5}Sn_{0.5}I_3$, and $CH_3NH_3SnI_3$ (**Figure 8** (a_1, b_1, c_1)). Photoluminescence is the emission of light observed when a material absorbs photons and re-emits them. This phenomenon is crucial in understanding the optoelectronic properties of these perovskite compounds, which have gained immense attention for their potential applications in solar cells and other electronic devices [33]. The data in the curves highlights the change in PL intensity peaks at different temperatures to 110 K to 300 K (**Figure 9** (a_2, b_2, c_2)).

We observe in **Figure 9** (a_2, b_2, c_2) that the PL intensity peaks increase as the temperature increases. This behavior is consistent with the general trend

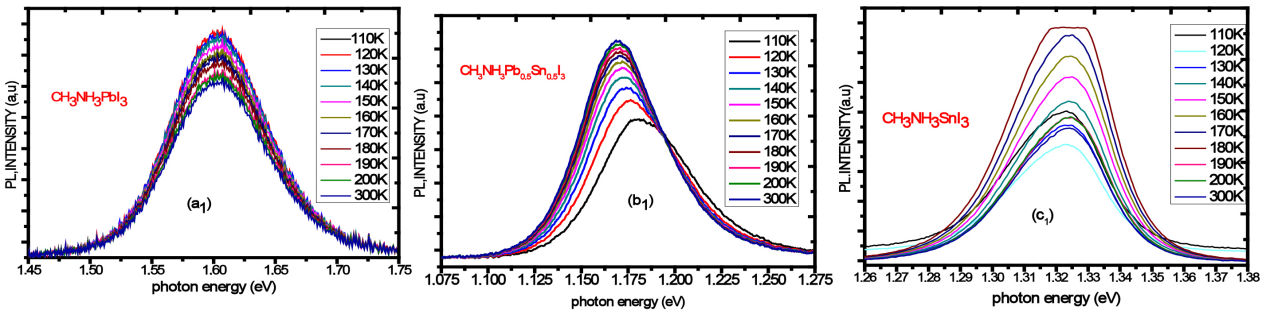

Figure 8. Curves of photoluminescence intensity of three materials.

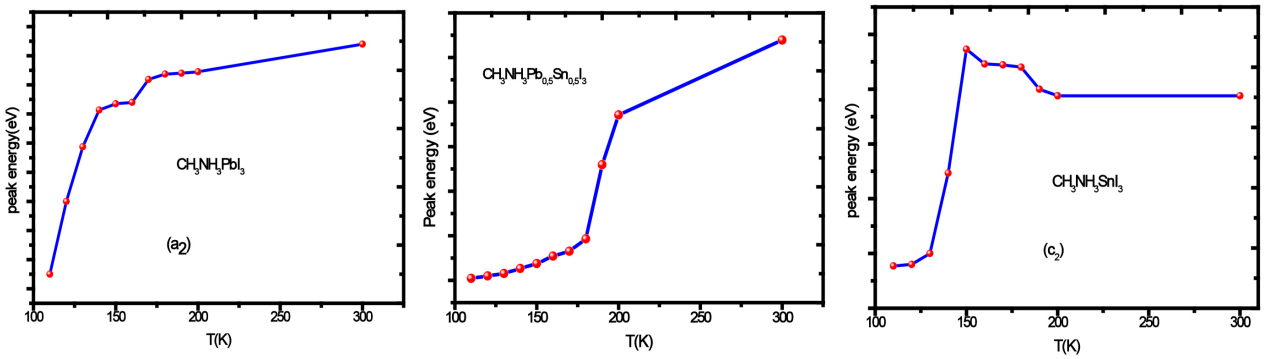

Figure 9. Curves of PL peaks.

observed in many semiconductor materials. At higher temperatures, more energy is available for electronic transitions, leading to enhanced photon emission and subsequently higher PL intensity. The temperature-dependent increase in PL intensity signifies the thermal excitation of electrons to higher energy states, followed by their relaxation to lower energy states with photon emission. Comparing the three compounds $CH_3NH_3PbI_3$, $CH_3NH_3Pb_{0.5}Sn_{0.5}I_3$, and $CH_3NH_3SnI_3$, it's evident that they exhibit different PL intensity behaviors. The energy values of the photoluminescence peaks decrease with increasing temperature. This decrease is more pronounced with doped perovskite (x = 0.5) but very slight with undoped perovskites ($CH_3NH_3PbI_3$ and $CH_3NH_3SnI_3$). This variation occurs around the gap energies of each material. The variation of the energy gap with temperature depends on the perovskite material and on its specific chemical composition, crystalline symmetry and other intrinsic properties of the material.

On the other hand, $CH_3NH_3Pb_{0.5}Sn_{0.5}I_3$ consistently shows intermediate PL intensity values, falling between $CH_3NH_3SnI_3$ and $CH_3NH_3PbI_3$. This indicates that the introduction of Sn into the perovskite structure, partially replacing Pb, has a moderate impact on the photoluminescence properties. The differences in atomic radii and electronic properties between Pb and Sn could influence the band structure and charge carrier dynamics, affecting the observed PL intensities.

The lead-based perovskite compound $CH_3NH_3PbI_3$, exhibits the lowest PL intensity peaks among the three compounds at both temperatures. This result might be attributed to the relatively larger atomic size of Pb compared to Sn, which could affect the crystalline structure and electronic properties, leading to less efficient charge transport and recombination. Additionally, lead-based perovskites have been known to exhibit some instability issues at higher temperatures, potentially contributing to the lower PL intensity observed.

The shift of the photoluminescence peak towards lower energies in the perovskite $CH_3NH_3Pb_{0.5}Sn_{0.5}I_3$ can be elucidated through several key mechanisms. The partial substitution of lead (Pb) with tin (Sn) creates structural defects and heterogeneities, introducing additional energy levels within the bandgap. These defects foster intricate electron-hole interactions, leading to the formation of tightly bound excitons and emission of light at lower energies. Additionally, the strain induced by the substitution alters the crystalline lattice, modifying electronic properties and phonon dynamics. These electron-phonon interactions influence polarons and energy-shifted electronic transitions, contributing to the observed peak shift. In essence, the photoluminescence shift arises from a combination of defect-induced effects from the Pb-Sn alloy, intricate electron-hole interactions, and alterations in the electronic structure due to strain and electron-phonon interactions in perovskite $CH_3NH_3Pb_{0.5}Sn_{0.5}I_3$.

7. Morphology of Perovskite Thin Film

Various surface analysis techniques are used to check the quality, compactness

and properties of films. The electronic characteristics of surfaces can be significantly affected by the presence of surface inhomogeneities.

The equipment used is the ZEISS ULTRA 55 model, with the following detectors: SE2 secondary electron detector, secondary electron detector, ASB backscattered electron detector, ESB backscattered electron detector, energy dispersive X-ray detector (EDS) and GEMINI technology.

The top view of the samples by Scanning Electron Microscope (SEM) informs us that the films obtained are weak in crystalline quality, inhomogeneous with a fairly high average as shown in **Figure 10**. The samples exhibit grains of different sizes. The surface of $CH_3NH_3PbI_3$ has a smoother surface than those of the other two compounds. The $CH_3NH_3Pb_{0.5}Sn_{0.5}I_3$ and $CH_3NH_3SnI_3$ layers have numerous pinholes, while $MAPbI_3$ has no pinhole. Pinholes can affect the uniformity and coverage of the perovskite layer, leading to variations in the absorption of light across the cell. Non-uniform absorption can result in uneven distribution of charge carriers and a decrease in overall efficiency [34].

With AFM images in **Figure 11**, we observe that the material $CH_3NH_3PbI_3$ exhibits a substantial thickness of 673 nm, coupled with a relatively high surface roughness of 13.1 nm. Despite the low roughness, the thickness of this compound is much higher than the other two. This roughness value provides a smooth surface, which is often desirable in thin-film technologies to minimise defects and improve device performance [35].

Moving on to $CH_3NH_3Pb_{0.5}Sn_{0.5}I_3$, this material demonstrates a considerably reduced thickness of 166.33 nm, accompanied by a lower surface roughness of 5.15 nm. The weakness of this film allows it to be used in the production of thin-film solar cells, where it is essential to minimise the use of materials or to obtain a more flexible and lighter structure. The reduced roughness further suggests that this material may offer improved surface quality, potentially making it advantageous for devices that require enhanced precision or efficiency. Lastly, $CH_3NH_3SnI_3$ falls between the other two materials in terms of both thickness and roughness. With a thickness of 464 nm and a roughness of 10.7 nm, it presents a middle ground between the extremes observed in $CH_3NH_3PbI_3$ and $CH_3NH_3Pb_{0.5}Sn_{0.5}I_3$. The differences in thickness and roughness among these materials can be attributed to variations in their chemical compositions and crystalline structures. The introduction of tin (Sn) in $CH_3NH_3Pb_{0.5}Sn_{0.5}I_3$, for instance, might influence the film's growth and properties, leading to a thinner and smoother layer compared to $CH_3NH_3PbI_3$.

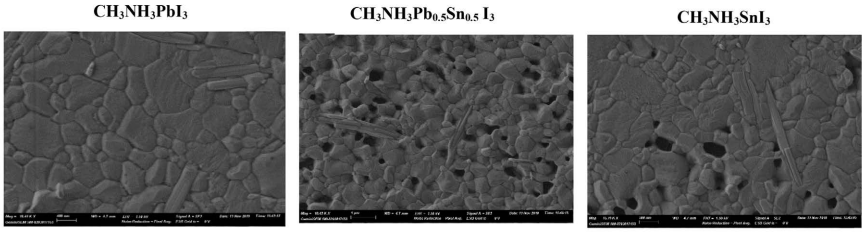

Figure 10. SEM images of perovskite films.

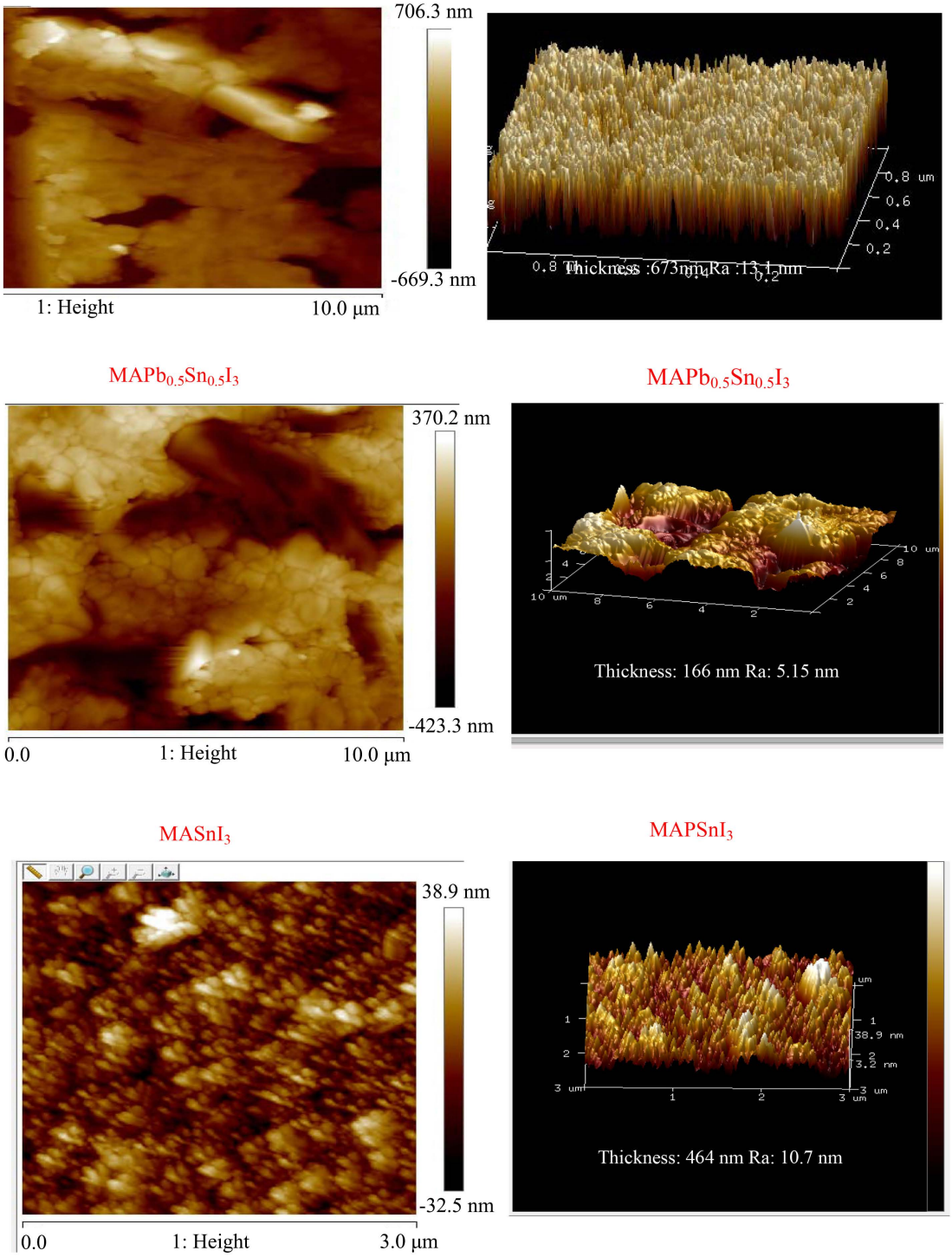

Figure 11. AFM images of perovskite films.

It should be noted that the values obtained are critical parameters in the optimisation of thin-film technologies. Achieving the right balance between thickness and roughness is crucial to the performance of devices such as solar cells, where film thickness influences light absorption and surface quality has an impact on charge carrier mobility [36].

8. Quantum Efficiency (QE)

As the tin content increases, there is a tendency for the quantum efficiency to increase, particularly at longer wavelengths (**Figure 12**). This trend suggests that there is an improvement in the absorption and generation of charge carriers with the incorporation of tin. The quantum efficiency varies considerably with the wavelength of the incident light. At shorter wavelengths (e.g. 450 nm), the quantum efficiency is generally lower for all materials. This could be because the energy of the incident photons is insufficient to generate charge carriers efficiently. The highest quantum efficiency values are often observed at wavelengths where the absorption of the material is also high.

For example, values are generally highest in the range 530 nm to 650 nm, indicating the maximum absorption range of these perovskite materials. At different wavelengths, different materials show varying quantum efficiency values. This suggests that each material has a unique absorption and charge generation profile. For example, at 570 nm, $MASnI_3$ shows the highest Quantum Efficiency, while at shorter wavelengths, $MAPbI_3$ performs better. $MAPb_{0.5}Sn_{0.5}I_3$ has slightly higher efficiency than other variations around the 490 nm mark but dips around 530 nm. The data showcases the effect of changing the composition of perovskite materials by substituting lead with tin in different ratios. This variation impacts the material's ability to absorb and convert light into electricity. The differences in Quantum Efficiency emphasize the importance of choosing the right material composition for specific applications. For instance, if a solar cell is designed to operate in a certain wavelength range, the appropriate material composition can be selected to maximize its efficiency in that range [24].

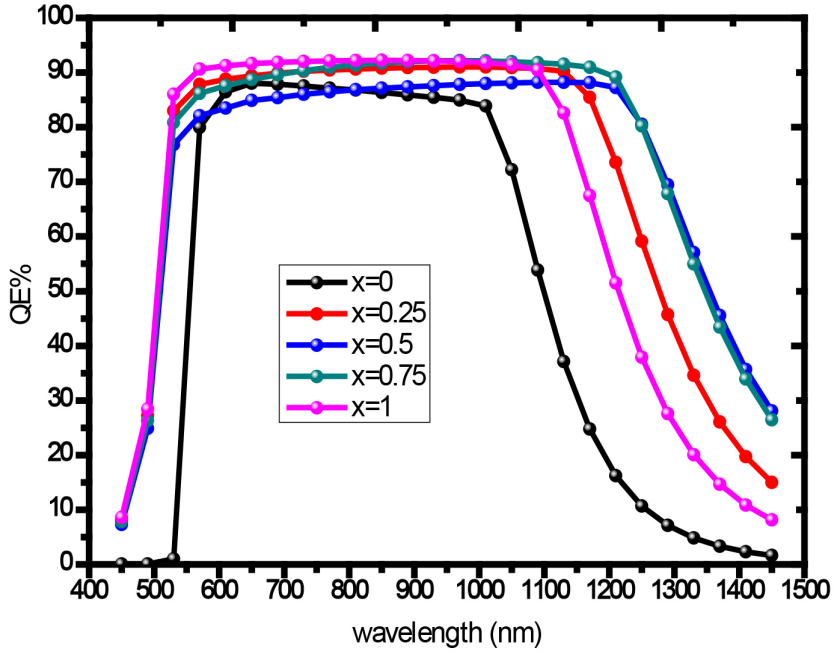

Figure 12. Curves of Quantum Efficiency (QE).

9. Conclusions

The substitution of toxic lead with tin in the fabrication of perovskite solar cells, specifically in the $MAPbI_3$ structure, has shown promising results with improved efficiency values. This shift towards more environmentally friendly and sustainable materials addresses concerns about the toxicity of lead and opens up new possibilities for the development of efficient and eco-friendly solar technologies.

The initial efficiency of $MAPbI_3$ was recorded at 22.49%, which served as the baseline for comparison with subsequent tin-substituted compositions. The introduction of tin into the perovskite structure, as seen in $MAPb_{0.5}Sn_{0.5}I_3$, resulted in a notable increase in efficiency to 23.00%. This enhancement suggests that tin, as a lead substitute, contributes positively to the optoelectronic properties of the perovskite material, leading to improved performance in solar cell applications.

Further exploration of the tin substitution strategy revealed that varying the tin content within the perovskite structure influences the overall efficiency of the solar cells. $MAPb_{0.5}Sn_{0.5}I_3$ exhibited a higher efficiency of 23%, showcasing the tunability of the material and the potential for optimizing the composition for even better performance. This result supports the idea that precise control over the composition can yield perovskite solar cells with superior properties, making them competitive with traditional solar cell technologies.

Moreover, the composition $MAPb_{0.25}Sn_{0.75}I_3$ demonstrated an efficiency of 22.61%, reinforcing the potential of tin as a viable alternative to lead in perovskite solar cells. The consistent high efficiency values across different tin concentrations indicate the robustness of this substitution strategy and its reliability in achieving improved performance.

In comparison to the lead-containing $MAPbI_3$, the tin-only perovskite $MASnI_3$ also exhibited a commendable efficiency of 22.38%. This result highlights the stand-alone efficiency capabilities of tin in a perovskite structure, affirming its suitability as a lead replacement. The success of $MASnI_3$ suggests that tin-based perovskites can be explored independently, providing a pathway for the development of lead-free perovskite solar cells with competitive efficiencies.

The ecological implications of these results are significant. The elimination of toxic lead from perovskite solar cells contributes to the reduction of environmental pollution and potential health risks associated with lead exposure. The development of lead-free perovskite solar cells aligns with the global shift towards sustainable and environmentally conscious technologies, marking a crucial step in the advancement of renewable energy.

It is essential to acknowledge that while the efficiencies reported in this study are promising, further research is needed to address potential challenges such as stability, scalability, and long-term performance. The field of perovskite solar cells is dynamic, with ongoing efforts to enhance material properties and manufacturing processes. Continued investigation into the optimization of tin-substituted perovskites, alongside advancements in device architecture and fabrication techniques, will contribute to the realization of efficient, lead-free perovskite solar cells for widespread commercial use.

Conflicts of Interest

The authors declare no conflicts of interest regarding the publication of this paper.

References

[1] Jäger-Waldau, A. (2011) Photovoltaics: Status and Perspectives until 2020. *Green*, **1**, 277-290. https://doi.org/10.1515/green.2011.027

[2] Edenhofer, O., Pichs-Madruga, R. and Sokona, Y. (2011) Renewable Energy Sources and Climate Change Mitigation. Special Report of the Intergovernmental Panel on Climate Change. Cambridge University Press, Cambridge. http://srren.ipcc-wg3.de/report https://doi.org/10.1017/CBO9781139151153

[3] Zillmer, J., *et al.* (2022) The Role of SnF_2 Additive on Interface Formation in All Lead-Free $FASnI_3$ Perovskite Solar Cells. *Advanced Functional Materials*, **32**, Article ID: 2109649.

[4] Peplow, M. (2023) A New Kind of Solar Cell Is Coming: Is It the Future of Green Energy? *Nature*, **623**, 902-905. https://doi.org/10.1038/d41586-023-03882-x

[5] Podapangi, S.K., *et al.* (2023) Green Solvents, Materials, and Lead-Free Semiconductors for Sustainable Fabrication of Perovskite Solar Cells. *RSC Advances*, **13**, 18165-18206. https://doi.org/10.1039/D3RA01692G

[6] Siegler, T.D., *et al.* (2022) The Path to Perovskite Commercialization: A Perspective from the United States Solar Energy Technologies Office. *ACS Energy Letters*, **7**, 1728-1734. https://doi.org/10.1021/acsenergylett.2c00698

[7] Mosconi, E., Umari, P. and De Angelis, F. (2015) Electronic and Optical Properties of Mixed Sn-Pb Organohalide Perovskites: A First Principles Investigation. *Journal of Materials Chemistry A*, **3**, 9208-9215. https://doi.org/10.1039/C4TA06230B

[8] Goyal, A., McKechnie, S., Pashov, D., Tumas, W., Van Schilfgaarde, M. and Stevanović, V. (2018) Origin of Pronounced Nonlinear Band Gap Behavior in Lead-Tin Hybrid Perovskite Alloys. *Chemistry of Materials*, **30**, 3920-3928. https://doi.org/10.1021/acs.chemmater.8b01695

[9] Liu, H., *et al.* (2023) Pure Tin Halide Perovskite Solar Cells: Focusing on Preparation and Strategies. *Advanced Energy Materials*, **13**, Article ID: 2202209. https://doi.org/10.1002/aenm.202202209

[10] Tilley, R.J.D. (2016) Perovskites: Structure-Property Relationships. Wiley, Chichester. https://doi.org/10.1002/9781118935651

[11] Quarti, C., *et al.* (2016) Structural and Optical Properties of Methylammonium Lead Iodide across the Tetragonal to Cubic Phase Transition: Implications for Perovskite Solar Cells. *Energy & Environmental Science*, **9**, 155-163. https://doi.org/10.1039/C5EE02925B

[12] Teng, Q., Shi, T.-T., Tian, R.-Y., Yang, X.-B. and Zhao, Y.-J. (2017) Role of Organic Cations on Hybrid Halide Perovskite $CH_3NH_3PbI_3$ Surfaces. *Journal of Solid State Chemistry*, **258**, 488-494. https://doi.org/10.1016/j.jssc.2017.10.029

[13] Ranjan, R., *et al.* (2023) SCAPS Study on the Effect of Various Hole Transport Layer on Highly Efficient 31.86% Eco-Friendly CZTS Based Solar Cell. *Scientific Reports*, **13**, Article No. 18411. https://doi.org/10.1038/s41598-023-44845-6

[14] Iftikhar, F.J., *et al.* (2021) Structural and Optoelectronic Properties of Hybrid Halide Perovskites for Solar Cells. *Organic Electronics*, **91**, Article ID: 106077.

https://doi.org/10.1016/j.orgel.2021.106077

[15] Yan, J., Song, X., Chen, Y. and Zhang, Y. (2020) Gradient Band Gap Perovskite Films with Multiple Photoluminescence Peaks. *Optical Materials*, **99**, Article ID: 109513. https://doi.org/10.1016/j.optmat.2019.109513

[16] Baikie, T., *et al.* (2013) Synthesis and Crystal Chemistry of the Hybrid Perovskite $(CH_3NH_3)PbI_3$ for Solid-State Sensitised Solar Cell Applications. *Journal of Materials Chemistry A*, **1**, 5628-5641. https://doi.org/10.1039/c3ta10518k

[17] Mitzi, D.B., Wang, S., Field, C.A., Chess, C.A. and Guloy, A.M. (1995) Conducting Layered Organic-Inorganic Halides Containing (110)-Oriented Perovskite Sheets. *Science*, **267**, 1473-1476. https://doi.org/10.1126/science.267.5203.1473

[18] Jung, H.S. and Park, N.-G. (2015) Perovskite Solar Cells: From Materials to Devices. *Small*, **11**, 10-25. https://doi.org/10.1002/smll.201402767

[19] Mandadapu, U., Vedanayakam, S.V., Thyagarajan, K., Reddy, M.R. and Babu, B.J. (2017) Design and Simulation of High Efficiency Tin Halide Perovskite Solar Cell. *International Journal of Renewable Energy Research*, **7**, 1604-1612.

[20] Mandadapu, U., Vedanayakam, S.V. and Thyagarajan, K. (2017) Simulation and Analysis of Lead Based Perovskite Solar Cell Using SCAPS-1D. *Indian Journal of Science and Technology*, **10**, 1-8.

[21] Baig, F. (2019) Numerical Analysis for Efficiency Enhancement of Thin Film Solar Cells. Universitat Politècnica de València, Valencia.

[22] Minemoto, T. and Murata, M. (2015) Theoretical Analysis on Effect of Band Offsets in Perovskite Solar Cells. *Solar Energy Materials and Solar Cells*, **133**, 8-14. https://doi.org/10.1016/j.solmat.2014.10.036

[23] Du, H.-J., Wang, W.-C. and Zhu, J.-Z. (2016) Device Simulation of Lead-Free $CH_3NH_3SnI_3$ Perovskite Solar Cells with High Efficiency. *Chinese Physics B*, **25**, Article ID: 108802. https://doi.org/10.1088/1674-1056/25/10/108802

[24] Ananda, W. (2017) External Quantum Efficiency Measurement of Solar Cell. 2017 15*th International Conference on Quality in Research* (*QiR*) : *International Symposium on Electrical and Computer Engineering*, Nusa Dua, 24-27 July 2017, 450-456. https://doi.org/10.1109/QIR.2017.8168528

[25] Jacobsson, T.J., Pazoki, M., Hagfeldt, A. and Edvinsson, T. (2015) Goldschmidt's Rules and Strontium Replacement in Lead Halogen Perovskite Solar Cells: Theory and Preliminary Experiments on CH_3 NH_3 SrI_3. *The Journal of Physical Chemistry C*, **119**, 25673-25683. https://doi.org/10.1021/acs.jpcc.5b06436

[26] Travis, W., Glover, E.N.K., Bronstein, H., Scanlon, D.O. and Palgrave, R.G. (2016) On the Application of the Tolerance Factor to Inorganic and Hybrid Halide Perovskites: A Revised System. *Chemical Science*, **7**, 4548-4556. https://doi.org/10.1039/C5SC04845A

[27] Chouhan, L., Ghimire, S., Subrahmanyam, C., Miyasaka, T. and Biju, V. (2020) Synthesis, Optoelectronic Properties and Applications of Halide Perovskites. *Chemical Society Reviews*, **49**, 2869-2885. https://doi.org/10.1039/C9CS00848A

[28] Zhang, L., *et al.* (2023) Advances in the Application of Perovskite Materials. *Nano-Micro Letters*, **15**, 177.

[29] Islam, M.R., *et al.* (2024) Tuning the Optical, Electronic, and Mechanical Properties of Inorganic Ca_3PCl_3 Perovskite via Biaxial Strain. *Journal of Physics and Chemistry of Solids*, **184**, Article ID: 111722. https://doi.org/10.1016/j.jpcs.2023.111722

[30] Zhang, Y. and Liu, H. (2019) Nanowires for High-Efficiency, Low-Cost Solar Photovoltaics. *Crystals*, **9**, Article No. 87. https://doi.org/10.3390/cryst9020087

[31] Du, T., *et al.* (2020) Light-Intensity and Thickness Dependent Efficiency of Planar Perovskite Solar Cells: Charge Recombination versus Extraction. *Journal of Materials Chemistry C*, **8**, 12648-12655. https://doi.org/10.1039/D0TC03390A

[32] Zhou, Y., *et al.* (2016) Doping and Alloying for Improved Perovskite Solar Cells. *Journal of Materials Chemistry A*, **4**, 17623-17635. https://doi.org/10.1039/C6TA08699C

[33] Manser, J.S., Christians, J.A. and Kamat, P.V. (2016) Intriguing Optoelectronic Properties of Metal Halide Perovskites. *Chemical Reviews*, **116**, 12956-13008. https://doi.org/10.1021/acs.chemrev.6b00136

[34] Jamal, M.S., *et al.* (2018) Fabrication Techniques and Morphological Analysis of Perovskite Absorber Layer for High-Efficiency Perovskite Solar Cell: A Review. *Renewable and Sustainable Energy Reviews*, **98**, 469-488. https://doi.org/10.1016/j.rser.2018.09.016

[35] Lewis, J. (2006) Material Challenge for Flexible Organic Devices. *Materials Today*, **9**, 38-45. https://doi.org/10.1016/S1369-7021(06)71446-8

[36] Ding, C., *et al.* (2022) Over 15% Efficiency PbS Quantum-Dot Solar Cells by Synergistic Effects of Three Interface Engineering: Reducing Nonradiative Recombination and Balancing Charge Carrier Extraction. *Advanced Energy Materials*, **12**, Article ID: 2201676. https://doi.org/10.1002/aenm.202201676